coatings

Supplementary Materials: Reduction of Surface Residual Lithium Compounds for Single-Crystal $LiNi_{0.6}Mn_{0.2}Co_{0.2}O_2$ via Al_2O_3 Atomic Layer Deposition and Post-Annealing

Jiawei Li [1], Junren Xiang [1], Ge Yi [1], Yuanting Tang [2], Huachen Shao [1], Xiao Liu [1,*], Bin Shan [2] and Rong Chen [1,*]

[1] State Key Laboratory of Digital Manufacturing Equipment and Technology, School of Mechanical Science and Engineering, Huazhong University of Science and Technology, Wuhan 430074, China; jiaweili@hust.edu.cn (J.L.); junrenxiang@hust.edu.cn (J.X.); geyigeyi@hust.edu.cn (G.Y.); shaohuachen@hust.edu.cn (H.S.)

[2] State Key Laboratory of Materials Processing and Die and Mould Technology, School of Materials Science and Engineering, Huazhong University of Science and Technology, Wuhan 430074, China; yuanting015@163.com (Y.T.); bshan@mail.hust.edu.cn (B.S.)

* Correspondence: xiaoliu@hust.edu.cn (X.L.); rongchen@mail.hust.edu.cn (R.C.)

Citation: Li, J.; Xiang, J.; Yi, G.; Tang, Y.; Shao, H.; Liu, X.; Shan, B.; Chen, R. Reduction of Surface Residual Lithium Compounds for Single-Crystal $LiNi_{0.6}Mn_{0.2}Co_{0.2}O_2$ via Al_2O_3 Atomic Layer Deposition and Post-Annealing. *Coatings* **2022**, *12*, 84. https://doi.org/10.3390/coatings12010084

Academic Editor: Alessio Lamperti

Received: 14 December 2021
Accepted: 6 January 2022
Published: 12 January 2022

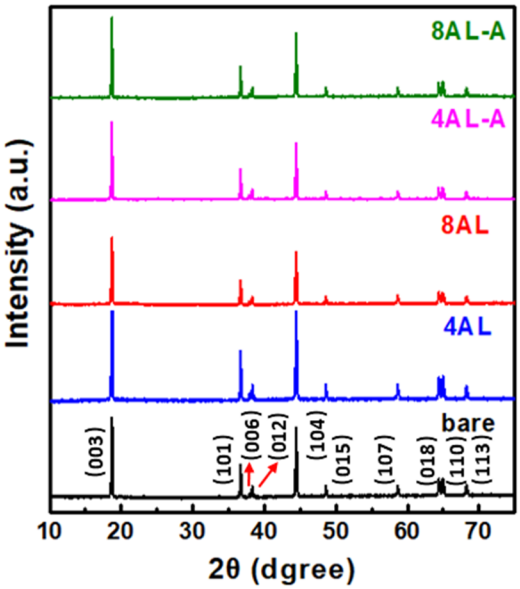

Figure S1. XRD patterns of bare, 4AL, 8AL, 4AL-A and 8AL-A NCM622 particles (the red arrows indicate diffraction peaks at 2theta of 37.9° and 38.3°). All samples show well-separated (006)/(012) peaks and (108)/(110) peaks, implying the typical α-$NaFeO_2$ layered structure. No extra peaks and no peak shift are detected in the XRD patterns of 4AL, 8AL, 4AL-A and 8AL-A samples, indicating that the ALD and post-annealing processes have no influence on the crystal structure of substrate materials.

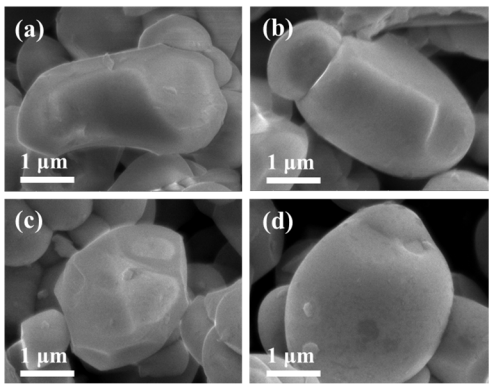

Figure S2. SEM images of (**a**) 4AL, (**b**) 8AL, (**c**) 4AL-A and (**d**) 8AL-A NCM622 particles. No obvious changes are observed in the morphologies after the ALD process or post-annealing.

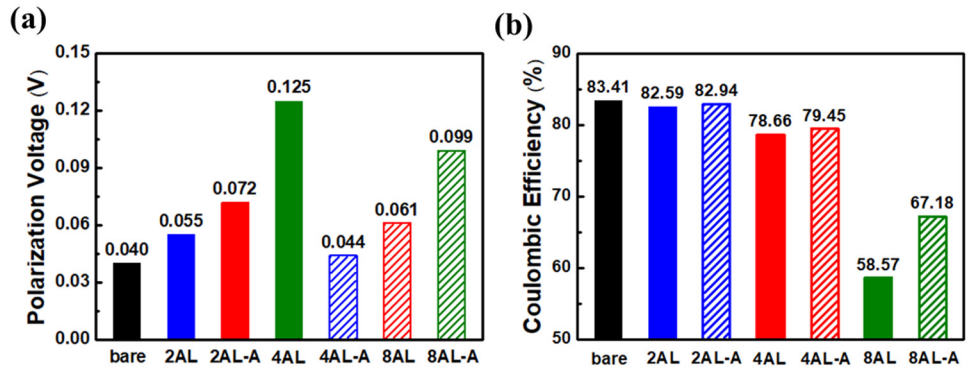

Figure S3. (**a**) Polarization voltages at the initial discharge stage and (**b**) initial coulombic efficiencies of bare, coated and annealed NCM622 cathodes. The post-annealing relieves the increment of polarization voltages and the decline of coulombic efficiencies.

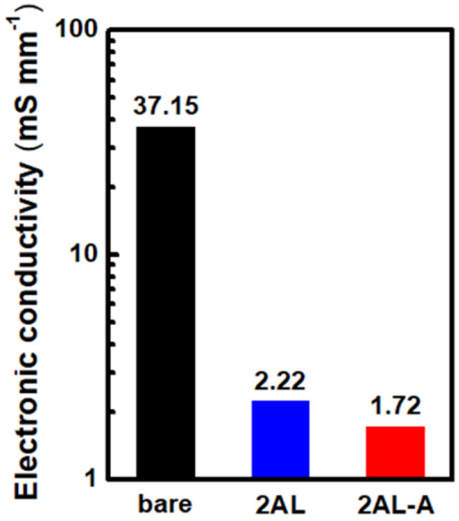

Figure S4. Electronic conductivities of bare, 2AL, and 2AL-A NCM622 particles. The electronic conductivity decreases after the Al_2O_3 ALD process and post-annealing process.

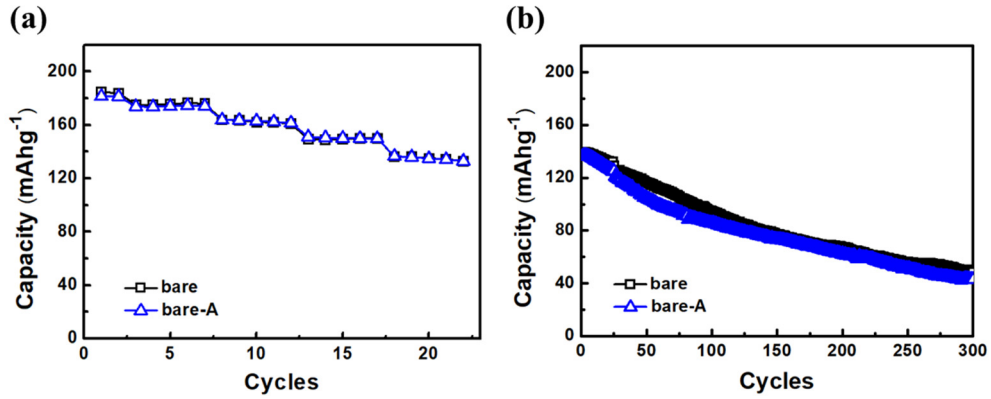

Figure S5. (**a**) Rate capability and (**b**) cycling stability of bare and bare-A NCM622 cathodes. These two cathodes show similar rate capability and cycling stability.

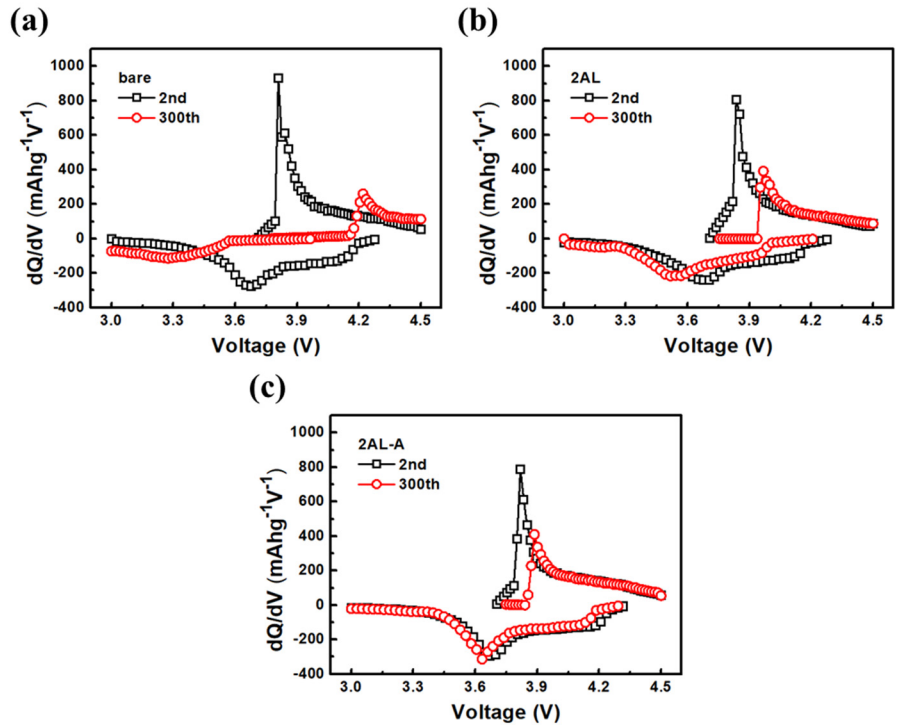

Figure S6. Differential capacity versus voltage profiles of (**a**) bare, (**b**) 2AL, and (**c**) 2AL-A NCM622 cathodes at the 2nd and 300th charge-discharge cycles. The 2AL-A NCM622 cathode well keeps the potential difference and intensity of redox peaks after cycles compared to others.

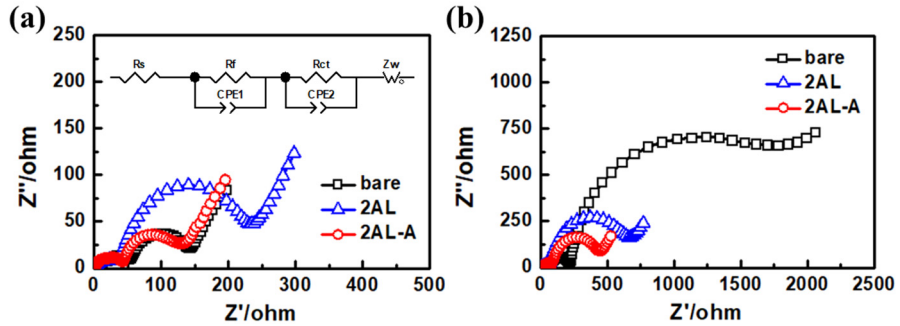

Figure S7. Electrochemical impedance spectra (EIS) of bare, 2AL, and 2AL-A NCM622 cathodes after the 2nd charge-discharge cycle (**a**) and the 300th charge-discharge cycle (**b**) at a charged state of 4.5V. The 2AL-A NCM622 cathode shows the lowest increment of R_{ct} compared to others.

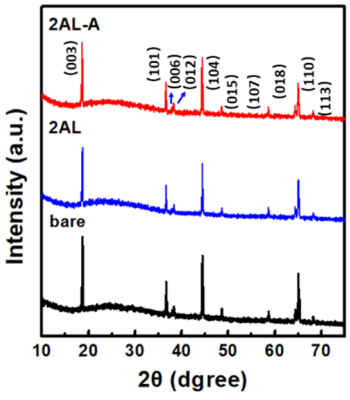

Figure S8. XRD patterns of bare, 2AL, and 2AL-A NCM622 cathodes before cycling (the blue arrows indicate diffraction peaks at 2theta of 37.9° and 38.3°). No obvious difference of crystal structures is observed among bare, 2AL, and 2AL-A NCM622 cathodes before cycling.

Table S1. Cycling stability of NCM622 cathodes at 1 C in this study compared to literature reports.

Years	Modification Strategy	Test Conditions	Capacity Retention	Capacity Loss Per Cycle
This work	Al_2O_3 ALD and post-annealing	3.0–4.5 V, 1 C	92.2 %, 300 cycles	0.026%
2021[1]	F doping	3.0–4.3 V, 1 C	94.5 %, 100 cycles	0.055%
2021[2]	Al and Zr doping	2.8–4.3 V, 1 C	92.1 %, 100 cycles	0.079%
2020[3]	ZrO_2 coating and post-annealing	2.8–4.5 V, 1 C	98.5 %, 150 cycles	0.01%
2021[4]	ZrW_2O_8 coating	2.8–4.5 V, 1 C	82.0 %, 100 cycles	0.18%
2019[5]	B doping	2.8–4.5 V, 1 C	96.1 %, 50 cycles	0.078%
2021[6]	Li-Si-O coating	3.0–4.5 V, 1 C	90.6 %, 100 cycles	0.094%
2021[7]	H_3BO_3 treatment	3.0–4.5 V, 1 C	88.5 %, 200 cycles	0.058%
2018[8]	Al_2O_3 and $LiAlO_2$ coatings	2.7–4.5 V, 0.2 C	84.5%, 100 cycles	0.155%

References

1. Huang, X.; Zhang, P.; Liu, Z.; Ma, B.; Zhou, Y.; Tian, X. Fluorine Doping Induced Crystal Space Change and Performance Improvement of Single Crystalline $LiNi_{0.6}Co_{0.2}Mn_{0.2}O_2$ Layered Cathode Materials. *ChemElectroChem* **2021**, *8*, 1–7, doi:10.1002/celc.202100756.
2. Feng, Z.; Zhang, S.; Rajagopalan, R.; Huang, X.; Ren, Y.; Sun, D.; Wang, H.; Tang, Y. Dual-Element-Modified Single-Crystal $LiNi_{0.6}Co_{0.2}Mn_{0.2}O_2$ as a Highly Stable Cathode for Lithium-Ion Batteries. *ACS Appl Mater Interfaces* **2021**, *13*, 43039–43050, doi:10.1021/acsami.1c10799.
3. Bao, W.; Qian, G.; Zhao, L.; Yu, Y.; Su, L.; Cai, X.; Zhao, H.; Zuo, Y.; Zhang, Y.; Li, H.; et al. Simultaneous Enhancement of Interfacial Stability and Kinetics of Single-Crystal $LiNi_{0.6}Mn_{0.2}Co_{0.2}O_2$ through Optimized Surface Coating and Doping. *Nano Lett* **2020**, *20*, 8832–8840, doi:10.1021/acs.nanolett.0c03778.
4. Xu, S.; Jing, N.; Hao, H.; Wang, M.; Wang, Z.; Yang, L.; Wang, G.; Chen, J.; Wang, G. Enhanced Electrochemical Performance of $LiNi_{0.6}Co_{0.2}Mn_{0.2}O_2$ by a Negative-Thermal-Expansion Material at Elevated Temperature. *Energy Technology* **2021**, *9*, doi:10.1002/ente.202100183.
5. Huang, B.; Yang, X.; Xu, G.; Wang, M.; Gu, Y. Boron-doped single crystal $LiNi_{0.6}Mn_{0.2}Co_{0.2}O_2$ with improved electrochemical performance for lithium-ion batteries. *Ionics* **2019**, *25*, 5819–5827, doi:10.1007/s11581-019-03166-3.
6. Li, G.; You, L.; Wen, Y.; Zhang, C.; Huang, B.; Chu, B.; Wu, J.H.; Huang, T.; Yu, A. Ultrathin Li-Si-O Coating Layer to Stabilize the Surface Structure and Prolong the Cycling Life of Single-Crystal $LiNi_{0.6}Co_{0.2}Mn_{0.2}O_2$ Cathode Materials at 4.5 V. *ACS Appl Mater Interfaces* **2021**, *13*, 10952–10963, doi:10.1021/acsami.0c22356.
7. Wang, W.; Wu, L.; Li, Z.; Huang, K.; Chen, Z.; Lv, C.; Dou, H.; Zhang, X. Stabilization of a 4.7 V High-Voltage Nickel-Rich Layered Oxide Cathode for Lithium-Ion Batteries through Boron-Based Surface Residual Lithium-Tuned Interface Modification Engineering. *Chemelectrochem* **2021**, *8*, 2014–2021, doi:10.1002/celc.202100125.
8. Liu, W.; Li, X.; Xiong, D.; Hao, Y.; Li, J.; Kou, H.; Yan, B.; Li, D.; Lu, S.; Koo, A.; et al. Significantly improving cycling performance of cathodes in lithium ion batteries: The effect of Al_2O_3 and $LiAlO_2$ coatings on $LiNi_{0.6}Co_{0.2}Mn_{0.2}O_2$. *Nano Energy* **2018**, 44, 111–120, doi:10.1016/j.nanoen.2017.11.010.